Journal of Experimental Nanoscience
Publication details, including instructions for authors and subscription information:
http://www.informaworld.com/smpp/title~content=t716100757

Polymer assisted preferential growth of PbS and PbS:Mn nanorods: structural and optical properties

A. R. Mandal[a]; S. K. Mandal[a]
[a] Department of Physics, Visva-Bharati, Santiniketan-731 235, India

To cite this Article Mandal, A. R. and Mandal, S. K.(2007) 'Polymer assisted preferential growth of PbS and PbS:Mn nanorods: structural and optical properties', Journal of Experimental Nanoscience, 2: 4, 257 — 267
To link to this Article: DOI: 10.1080/17458080701753736
URL: http://dx.doi.org/10.1080/17458080701753736

Journal of Experimental Nanoscience,
Vol. 2, No. 4, December 2007, 257–267

Taylor & Francis
Taylor & Francis Group

Polymer assisted preferential growth of PbS and PbS:Mn nanorods: structural and optical properties

A. R. MANDAL and S. K. MANDAL*

Department of Physics, Visva-Bharati, Santiniketan-731 235, India

(*Received September 2007; in final form October 2007*)

We report here the structural and optical properties of PbS and PbS:Mn nanorods (diameter 30–80 nm) grown in a polymer (polypyrrole) matrix. X-ray diffraction data of nanorods clearly reveals preferential growth of PbS nanorods with a strong lattice distortion from a bulk cubic to tetragonal one. The strain introduced lattice distortion is inherent to the growth process and strongly depends on polymer concentration. The polymer concentration is found to play an important role in controlling the structural properties. The effect of Mn^{2+} incorporation into PbS lattice shows no appreciable change in the structural properties. Optical absorption behaviors in such PbS and PbS:Mn nanorods are also reported. The absorption peak energy shows blue-shift with increase in Mn^{2+} concentration to some critical value beyond which red-shift is observed.

Keywords: PbS; Nanorods; Lattice distortion; Optical absorption

1. Introduction

PbS belonging to the group of IV–VI compounds is a widely used material for infrared detectors and tunable laser devices [1]. PbS has a direct band-gap of 0.41 eV at 300 K and strongly temperature dependent. It is further characterized by a complex band structure. Both the conduction and valence band show multiple-valley structure with the band extrema occurring at L-points of the Brillouin zone. Due to the small energy gap, k.p interaction (spatial variation of band energies and inter-band momentum matrix elements) is quite dominant in PbS band structure [2]. The k.p interaction between the lowest conduction band level and nearest degenerate valence levels (heavy hole, light hole bands etc.) is manifested in terms of formation of sub-bands, spatial dependent change in electronic effective mass and non-parabolic shape in energy-band structure. On the other hand, Pb being a heavier element leads to strong spin-orbit interaction. This suggests that the presence of any (para)-magnetic species

*Corresponding author. Email: sk_mandal@hotmail.com

Journal of Experimental Nanoscience
ISSN 1745–8080 print/ISSN 1745–8099 online
http://www.tandf.co.uk/journals
DOI: 10.1080/17458080701753736

may strongly modify their electronic and magnetic properties [2]. Paramagnetic doping (Mn^{2+}, Eu^{2+}, Fe^{3+} etc.) in wide band-gap II–VI and III–V compound has been largely explored to tailor their physical properties both in bulk and nanostructures. Large interest lies in such doped II–VI and III–V semiconductor nanostructures for the realization of photonic and spintronic devices [3–5]. However, the effect of paramagnetic doping in IV–VI compounds in reduced dimensions is scarcely addressed. Pascher *et al*. [6] had suggested that the presence of paramagnetic ion in lead salts (PbS, PbTe, PbSe, etc.) can strongly modify their electronic and magnetic behaviors. The IV–VI semiconductors have the intrinsic tendency to grow non-stoichiometrically which gives rise to a high concentration of native defects distributed over the crystal volume. The presence of magnetic ions deviates the system from the free carrier behaviors through sp-d exchange interaction between the localized carriers and itinerant carriers. Our interest lies in the synthesis of IV–VI (PbS here) semiconductor nanostructures doped with Mn^{2+}, and unveils their structural, optical and importantly magnetic properties. The synthesis of such PbS nanorods may widen the possibilities of creating functional two-dimensional or three-dimensional nanostructures and devices. Also, from the infra-red electroluminescent device point of view, nanocomposites of PbS and polymer in solid state are found to exhibit photoluminescence quantum efficiency as high as ~12% [7].

Size-tunable PbS quantum dots are synthesized and studied by many authors through a solution based organometallic route or in a water-based solution [8–10]. The PbS quantum dots are found to exhibit blue-shifted absorption peaks as an indication of a strong quantum confinement effect, and non-linear optical properties. Besides quantum dots, PbS in their nanorod structures are also reported [11–12]. However, subsequent doping with paramagnetic ions in such PbS nanorods is not reported to date. Here, we synthesize both undoped and Mn^{2+} doped PbS nanorods in polymer matrix and correlate their structural and optical properties. We use polypyyrole (PPY) amongst the variety of polymers because of its high environmental stability.

2. Experimental

The polymerization of pyrrole and the co-deposition of PbS in the form of nanorods are accomplished by a simple wet chemical technique. The procedure takes place first by exchanging Pb^{2+} ions into the pyrrole and then reacting with S^{2-}. A solution of $Pb(NO_3)^2$ (purified, Loba Chemie, India) is prepared. Ethanol (GR, Jiangsu Huaxi, China) dried over activated molecular sieve zeolite 4A and distilled water is used as the solvent. The volume ratio of water and alcohol is maintained 1:5 throughout to prepare the solution. Then different amounts of pyrrole (SRL, India) are added into the solution under rapid stirring to obtain various pyrrole concentrations, 5, 10 and 15wt% respectively. For sulfur (S^{2-}) precursor, we use sodium thiosulfate ($Na_2S_2O_3$, $5H_2O$, purified, Merck, India) dissolved in distilled water. Both the solutions are continuously stirred for 2 hours keeping the bath temperature ~60°C. In the precursors, the molar ratio of lead and sulfur is maintained as Pb:S = 1:1 to obtain the required stoichiometry in the derived lead sulfide embedded in polypyrrole. Finally, sulfur solution is slowly added to the lead (Pb^{2+}) solution keeping the bath temperature the same. This results

instantly in the formation of PbS within the polypyrrole matrix. The precipitate is washed in distilled water three times, filtered and dried at room temperature in a vacuum. The ion-exchange reaction mechanism for the formation PbS nanorods in polypyrrole can be proposed in the following way:

$$Pb^{2+} + (PPY)_{complex} \rightarrow Pb^{2+}(PPY)_{complex}$$

$$Na_2S_2O_3 \rightarrow Na^+ + SO_3^{2-} + S^{2-}$$

Finally, $Pb^{2+}(PPY)_{complex}$ reacts with $S^{2-}$to form PbS.

$$Pb^{2+}(PPY)_{complex} + S^{2-} \rightarrow (PbS)(PPY)_{complex} \downarrow$$

On the other hand, to synthesize Mn^{2+} doped PbS, different molar % of Pb^{2+} is substituted by Mn^{2+} in the lead solution through $Mn(CH_3COO)_2$, $4H_2O$ (extra pure, Loba Chemie, India). We thus prepare both, doped and Mn^{2+} doped, PbS in polypyrrole matrix with different Mn^{2+} concentrations (2, 4 and 6 mole%) corresponding to polypyrrole concentrations of 5, 10 and 15 wt%. Note the extent of doping in PbS lattice may differ from the above molar concentration of Mn^{2+} in starting solution.

3. Results and discussion

The surface morphology of PbS nanorods encapsulated in polypyrrole is characterized by scanning electron microscopy (SEM). Figure 1(a–c) depicts the surface morphology of PbS nanorods synthesized with pyrrole concentrations of 5, 10 and 15 wt% respectively. The figure clearly reveals that the concentration of pyrrole largely determines the growth and morphology of the nanorods. A representative TEM image along with corresponding selected area diffraction pattern (inset of figure 2) for PbS sample with 15 wt% polypyrrole is presented in figure 2. The diffraction spots are clearly indicative of the preferential growth of PbS nanorods. The average size (diameter D) of the nanorods as obtained from TEM images are found to be D (=2R, R being the radius) ~30 nm, 50 nm and 80 nm (with an estimated error of ±5 nm) for samples grown with 5, 10 and 15 wt% pyrrole, respectively. The nanorods are straight and have length ~2000 nm. Clearly, the monomer concentration plays an important role in determining the size of the nanorods. It can also be seen that the surface morphology becomes more non-uniform in the length and size of the nanorods as the pyrrole concentration increased to 15 wt%. The growth of the nanorods plausibly instigated by the elongation of PbS nanocrystals in a chain-like pattern, encapsulated by the polymer and finally giving the nanorod structures. It is reported earlier that very low concentration (depends upon the materials of study and synthesis process) of pyrrole gives rise to the formation of nanocrystals rather than nanorods. Many authors observe such initial nucleation of nanoclusters and their subsequent curling up into nanorod structures in polymer network earlier [12]. Further, as the pyrrole

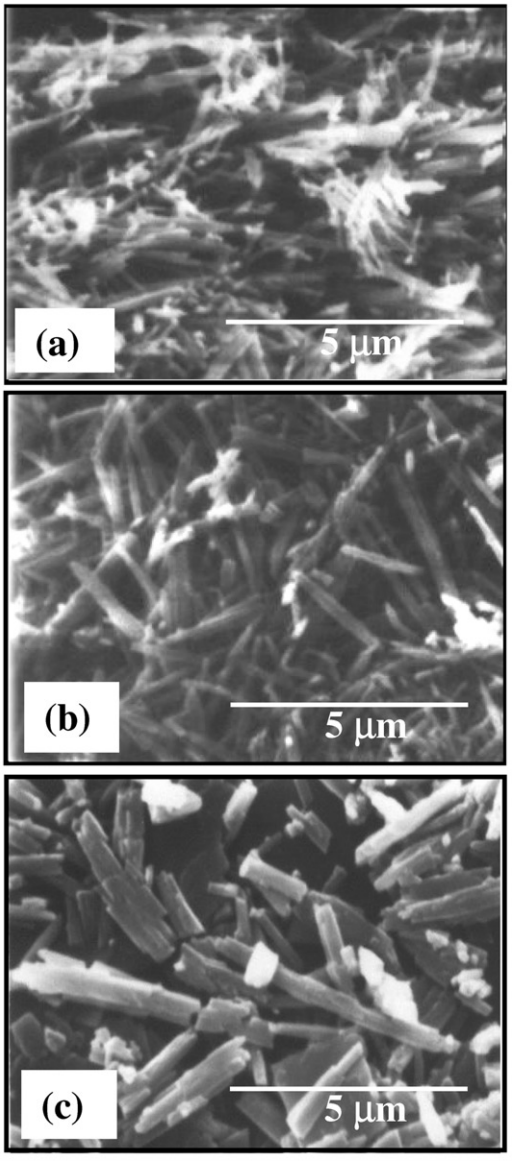

Figure 1. SEM images of PbS nanorods synthesized with polypyrrole concentrations: (a) 5 wt%, (b) 10 wt% and (c) 15 wt%.

concentration is increased beyond a critical value (here more than 10 wt%), the kinetics of growth is inhibited by the formation of non-uniform clustered growth. This can be the possible reason why the nanorods in figure 1(c) grown at higher pyrrole concentration becomes less uniform in size and length along with the presence of nanoclusters. We mention that similar morphological structures are obtained while adding Mn for the synthesis of PbS:Mn nanorods. Addition of Mn^{2+} did not make any

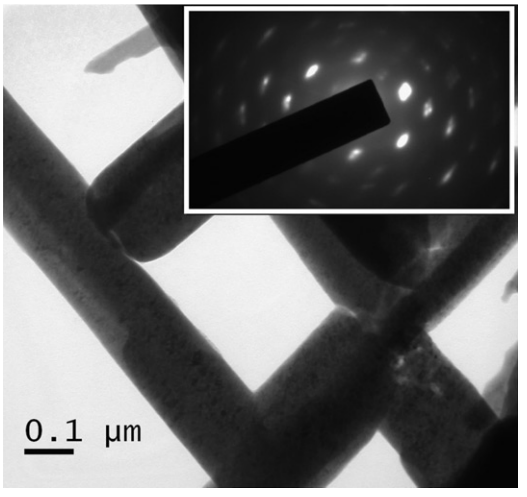

Figure 2. TEM image of a representative sample with PbS nanorods synthesized with polypyrrole concentrations 15 wt%. Inset shows the corresponding diffraction pattern.

appreciable change in the growth process described above. The polymerization of pyrrole is confirmed by the FTIR transmission spectra of the samples. Figure 3 shows the FTIR transmission spectra of PbS samples with Mn^{2+} concentrations 0–6% corresponding to 5 wt% polypyyrole. The spectra clearly indicate the various stretching modes of vibration ($>C=C<$, N–H, $>C$–H, $>C=N$) of polypyrrole in the region 1000–1500 cm^{-1} and the band centered at 3500 cm^{-1} indicates the N–H stretch in polypyrrole [13–14]. We used atomic absorption spectroscopy (AAS) to confirm Mn doping PbS. The samples are washed several times in a mixture of ethanol and water and tested with AAS which gives no signature of elemental Mn present in the doped PbS samples.

The X-ray diffraction (XRD) spectra for a representative sample (5 wt% pyrrole) with different Mn^{2+} concentrations are given in figure 4. The diffraction peaks position and their distribution in intensity significantly differ from that of bulk fcc lattice of PbS powder. We find that the most intense peak corresponds to (220) lattice plane instead of (200) of bulk PbS (galena) pattern. Clearly, strong (220) diffraction peak is a characteristic of the preferential orientation of the lattice planes. Such preferred orientation is of course dependent on the growth mechanism and is observed for PbS nanorods and needles in polymer [12]. The significant shift ($>1^0$) in the peak position of (220) plane compared to the bulk one can be attributed to the strain developed during the formation of rods within the polymer network. The size (s) of the nanorods is not small enough to cause any significant shift in the diffraction angle in our synthesized nanorods. The observation of peak-shift can be interpreted as a strain induced distortion of the fcc lattice into a tetragonal one. On a closer look into the XRD spectra, we find that, although the most intense (220) d spacing shows contraction, other peaks like (111) and (200) exhibit increase in d values. Considering the (220) plane, we obtain the lattice contraction by 2.77%. On the other hand, calculation based on (111) plane indicates an expansion of the lattice as large as ~5.72%.

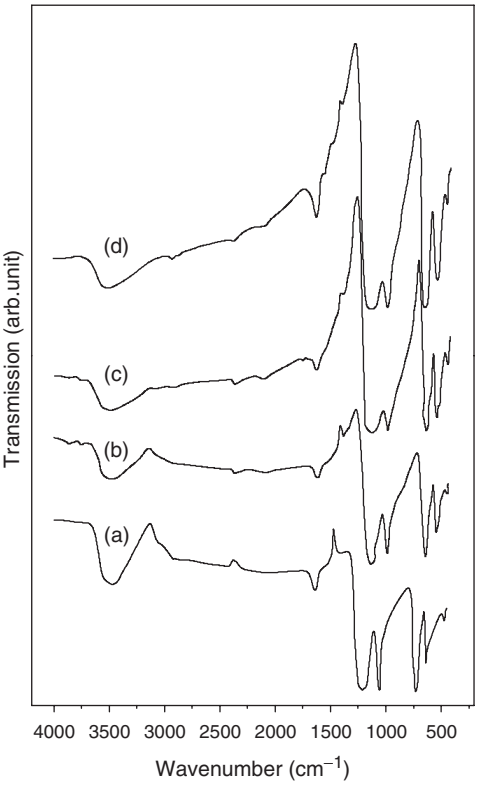

Figure 3. FTIR spectra of PbS nanorods synthesized at a polypyrrole concentration 5 wt% with different % molar concentration of Mn^{2+}: (a) 0; (b) 2; (c) 4 and (d) 6.

Clearly, XRD spectra reveal a strong distortion of the PbS nanorod structures confined in polypyrrole. Considering the PbS lattice constant ~5.9413 Å, we find the a/c ratio for the tetragonal lattice ~1.08 (for undoped sample with pyrrole concentration 5 wt%). With increasing polymer concentration, reduction in peak intensity supports the fact that the nanorods undergo severe strain during growth. This is also reflected in the SEM micrograph (figure 1(c)) for samples with high pyrrole concentration that give fracture and breakage with uneven distribution of nanorods. Such lattice distortion is observed before for PbS and CdS quantum dots [15–16]. Their observation is attributed to the quantum size effect in quantum dots. In our case, the distortion cannot be ascribed to the size effect. The PbS nanorods, described here, are weakly (quantum)-confined and reasonably the strain associated in the nanorods is not due to size effect in origin. The strain is inherent to the growth process and dependent on the polymer concentration. To be mentioned, addition of Mn^{2+} in PbS growth did not make any appreciable change in the XRD spectra from that of undoped ($Mn^{2+} = 0$) one. We obtain similar results for all the samples grown with different pyrrole concentrations and their subsequent doping with Mn^{2+} (not shown here). Presence of some very low intense peaks observed in the XRD spectra can be indexed to the amorphous polypyrrole. The structural and morphological data lead us further to

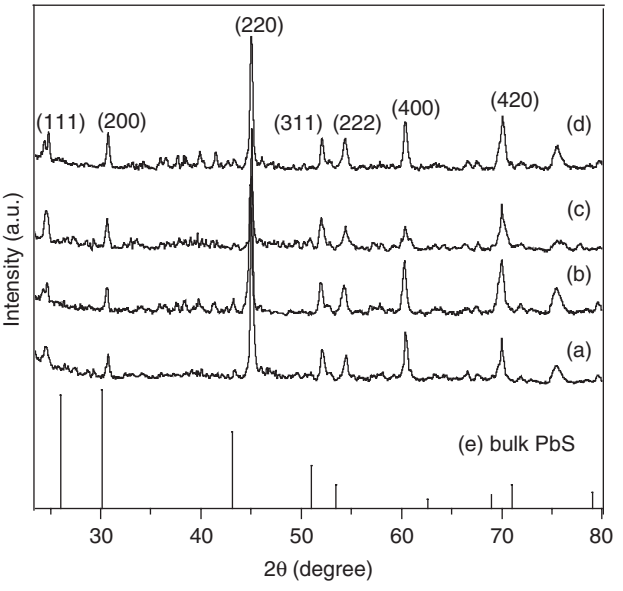

Figure 4. XRD spectra (top) of PbS nanorods synthesized at a polypyrrole concentration 5 wt% with different % molar concentration of Mn^{2+}: (a) 0; (b) 2; (c) 4 and (d) 6. The data are compared with bulk PbS given in (e).

investigate the plausible growth mechanism of nanorods. The mechanism is instigated by the self-assembly of nanoparticles by spontaneous adjustment along the linear chain of polymer templates. A schematic diagram of the growth process is illustrated in figure 5. In the early stage of nucleation, finer particles of PbS are formed (figure 5(a)). The presence of polypyrrole inhibits the agglomeration of nanoparticles into a larger one. Subsequently, under hydrothermal conditions, the finer particles are subjected to the crystallization process in a self-assembly fashion (can be seen stepwise through figure 5(b–d)). Preferential growth along the long polymer chain takes place between adjacent nanoparticles due to energy minimization. The various crystallographic planes having relatively higher free surface energy are more thermodynamically unstable. Adsorbing the polymer on their surface follows the energy minimization. In our case, (220) plane of PbS nanorods may have more ability to adsorb the polymer molecules. Therefore selective adsorption of polypyrrole on the specific site PbS eventually leads to the observed preferential growth along (220). The observed peak intensity profile for PbS nanorods therefore differs from that of bulk. Such preferential growth and peak intensity distributions different from that of bulk are observed for metal nanowires [17]. The polymer concentration and hydrothermal conditions therefore plays an important role in the whole growth process. With increasing polymer concentration, the connectivity of the polymer networks increases, giving rise to more twists and breakage of nanorods, hence generation of strain. Also, the nanorods in polymer can undergo severe strain during the drying or solvent evaporation stage as observed by others [12]. The strain occurs both along and across the growth direction of nanorods, presumably anisotropic in nature.

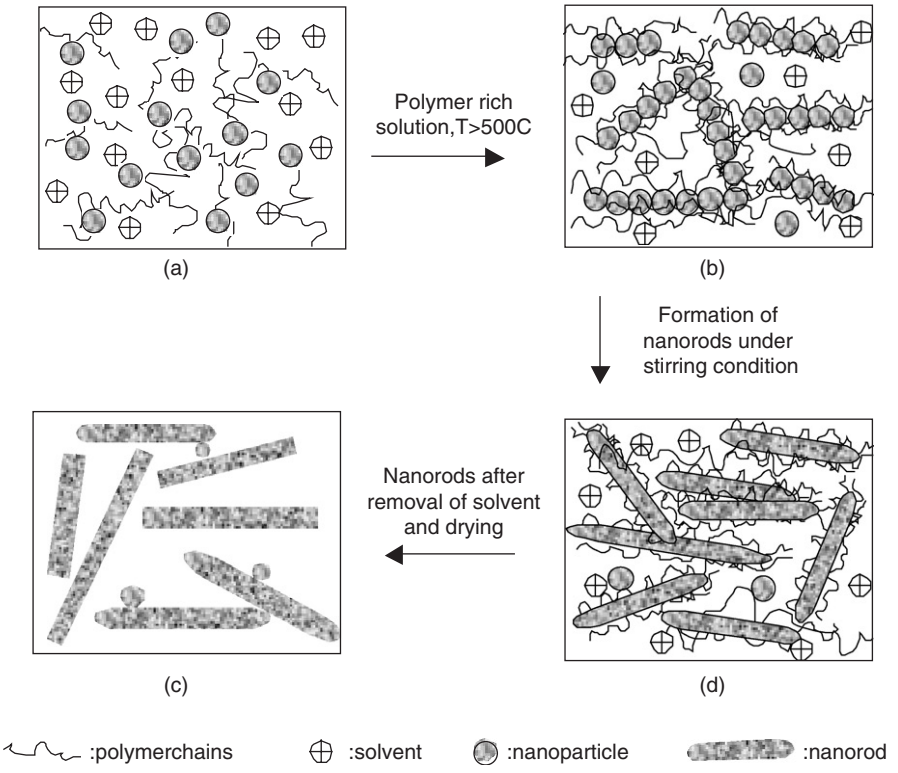

Figure 5. Schematic model for the growth of PbS nanorods in polymer (a): initial nucleation of PbS fine particles, (b)–(d): subsequent preferential growth of nanorods under suitable hydrothermal conditions and polymer rich solution.

We now look into the optical absorption spectra of both PbS and PbS:Mn nanorods, given in figure 6. At a given pyrrole concentration, we plot the absorption intensity with Mn^{2+} concentrations. The absorption peaks are broadened to some extent with increased polypyrrole concentrations because of a relatively broad size distribution of nanorods, as revealed by SEM morphologies. All the data clearly reveal that the incorporation of Mn^{2+} slightly influences the absorption peak maximum (corresponding to the band-gap absorption edge). The shift in absorption maximum peak energy with Mn^{2+} concentration is shown in figure 7. The data shows a small blue shift (10–15 meV) in peak energy compared to the undoped ($Mn^{2+} = 0$) one. It is also noted that the presence of excess Mn^{2+} concentration leads to red-shift in peak energy. The results retain the same characteristics for all the samples grown with different pyrrole concentrations. Indeed, the excitonic states are weakly confined, as expected. The size (D) of the nanorods is somewhat larger than the exciton Bohr radius $a_B \sim 20$ nm ($D \gg a_B$) for PbS. The optical data seems to be quite interesting as the paramagnetic ion in PbS influences the excitonic absorption spectrum besides magnetic properties. The increase in band-gap (blue-shift) was reported for semi-magnetic lead chalcogenides earlier and possibly arises due to the inter-band mixing phenomena through s.d interaction between band electrons and the localized carriers associated

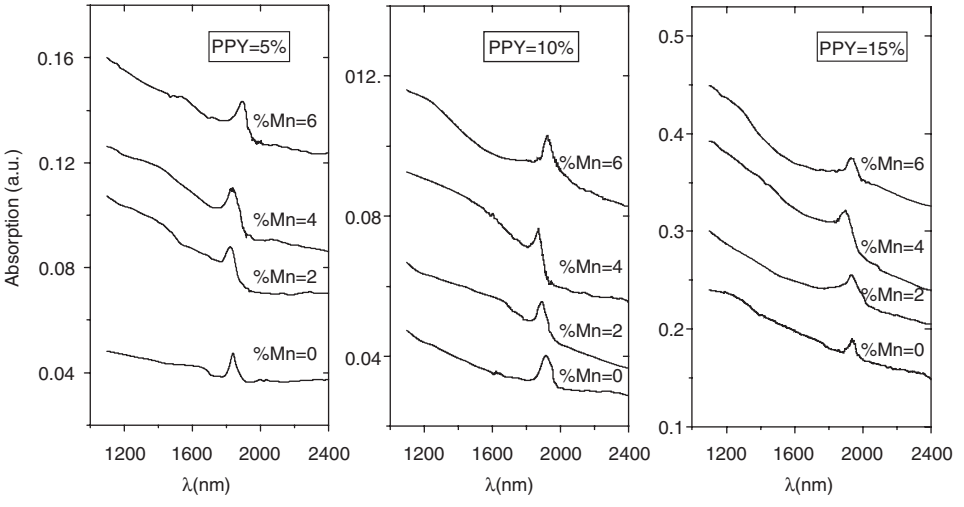

Figure 6. Optical absorption spectra of Mn^{2+} doped (molar concentration 0 to 6%) PbS nanorods corresponding to different concentration of polypyrrole: 5 wt%, 10 wt% and 15 wt%.

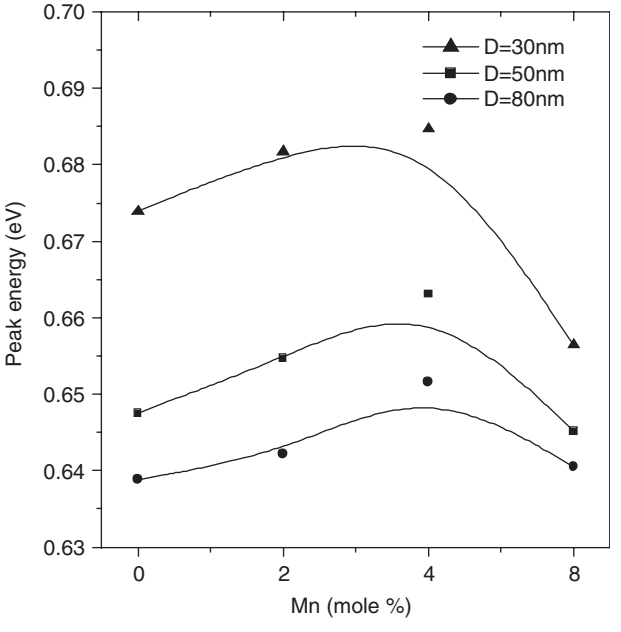

Figure 7. Shift of the optical absorption peak energy with different Mn^{2+} concentrations in PbS:Mn nanorods.

with Mn ions [2]. The red-shift possibly occurred (in presence of excess Mn^{2+} ions) when the Mn^{2+} resided in the host lattice in an interstitial position rather than as a substitution of Pb^{2+}. Also the clustering effect of Mn ions as observed for ZnS:Mn cannot be ruled out [18]. Effect of strain is also reflected in the absorption

spectra giving rise to more broadened absorption peaks with increase in polypyrrole concentrations that is consistent with the XRD data.

4. Conclusions

In conclusion, we report here the preferential growth of PbS and Mn^{2+} doped PbS nanorods in polypyrrole matrix. The nanorods suffer significant strain during the growth process which leads to strong lattice distortion of the bulk fcc PbS lattice to a tetragonal one. We find that addition of Mn^{2+} did not make any significant difference to the structural properties in the PbS nanorods synthesized here. However, slight blue shift can be observed in the optical absorption features while increasing the Mn^{2+} concentration to a moderate value ~4 mol%. Attempts to further increase the doping concentration of Mn^{2+} lead to a red-shift of the absorption peak maximum. The result can be interpreted as the Mn^{2+} occupies interstitial positions in the host PbS lattice, and clustering of Mn ions.

The authors acknowledge with thanks to CSIR, New Delhi, India for financial support and providing a Junior Research Fellowship to one of the authors (A.R.M.). Thanks to Prof. S. Chaudhuri, I.A.C.S., Kolkata-32 for providing SEM facilities.

References

[1] Y.I. Ravich, B.A. Efimov, I. Smornov. *Lead Chalcogenides*, Plenum Press, New York (1970).
[2] G. Bauer, H. Pascher, W. Zawadzki. Magneto-optical properties of semimagnetic lead chalcogenides. *Semicond. Sci. Tehnol.*, **7**, 703 (1992).
[3] S.A. Wolf, D.D. Awschalom, R.A. Buhrman, J.M. Daughton, S. von Molnár, M.L. Roukes, A.Y. Chtchelkanova, D.M.T. Reger. Spintronics: a spin-based electronics vision for the future. *Science*, **294**, 1488 (2001).
[4] S.J. Pearton, C.R. Abernathy, M.E. Overberg, G.T. Thaler, D.P. Norton, N. Theodoropoulou, A.F. Hebard, Y.D. Park, F. Ren, J. Kim, L.A. Boatner. Wide band gap ferromagnetic semiconductors and oxides. *J. Appl. Phys.*, **93**, 1 (2003).
[5] S.A. Chambersa, T.C. Droubaya, C.M. Wanga, K.M. Rossoa, S.M. Healdb, D.A. Schwartzc, K.R. Kittilstvedc, D.R. Gamelinc. Ferromagnetism in oxide semiconductors. *Materials Today* **9**, 28 (2006).
[6] H. Pascher, P. Rothlein, G. Bauer, M. von Ortenberg. Band structure of diluted magnetic $Pb_{1-x}Mn_xTe$: magneto-optical investigations and four-wave-mixing spectroscopy. *Phys. Rev. B.*, **40**, 10469 (1989).
[7] T.-W.F. Chang, A. Maria, P.W. Cyr, V. Sukhovatkin, L. Levina, E.H. Sargent. High near-infrared photoluminescence quantum efficiency from PbS nanocrystals in polymer films. *Synth. Met.*, **148**, 257 (2004).
[8] E.H. Sargent. Infrared quantum dots. *Adv. Mater.*, **17**, 515 (2005).
[9] S. Puvvada, S. Baral, G.M. Chow, S.B. Qadri, B.R. Ratna. Synthesis of palladium metal nanoparticles in the bicontinuous cubic phase of glycerol monooleate. *J. Am. Chem. Soc.*, **116**, 2135 (1994).
[10] Z. Hens, D. Vanmaekelbergh, E.J.A.J. Stoffels, H. van Kempen. Effect of crystal shape on the energy levels of zero-dimensional PbS quantum dots. *Phys. Rev. Lett.*, **88**, 236803 (2002).
[11] Z. Liu, J. Liang, D. Xu, J. Lu, Y. Qian. A facile chemical route to semiconductor metal sulfide nanocrystal superlattices. *Chem. Commun.*, **23**, 2724 (2004).
[12] S. Yang, S. Wang, K.K. Fung. One-dimensional growth of rock-salt PbS nanocrystals mediated by surfactant/polymer templates. *Pure Appl. Chem.*, **72**, 119 (2000).
[13] B. Tian, G. Zerbi. Lattice dynamics and vibrational spectra of polypyrrole. *J. Chem. Phys.*, **92**, 3886 (1990).
[14] S.K. Mandal, P. Dutta. Synthesis of DNA-Polypyrrole Nanocapsule. *J. Nanosci. Nanotechnol.*, **4**, 972 (2004).
[15] S.B. Qadri, J.P. Yang, E.F. Skelton, B.R. Ratna. Evidence of strain and lattice distortion in lead sulfide nanocrystallites. *Appl. Phys. Lett.*, **70**, 1020 (1997).

[16] Y. Wang, N. Herron. Quantum size effects on the exciton energy of CdS clusters. *Phys. Rev. B.*, **42**, 7253 (1990).
[17] H. Pan, H. Sun, C. Poh, Y. Feng, J. Lin. Single-crystal growth of metallic nanowires with preferred orientation. *Nanotechnology*, **16**, 1559 (2005).
[18] Y.H. Lee, D.H. Kim, B.K. Ju, M.H. Song, T.S. Hahn, S.H. Choh, M.H. Oh. Decrease of the number of the isolated emission center Mn^{2+} in an aged ZnS:Mn electroluminescent device. *J. Appl. Phys.*, **78**, 4253 (1995).